QUANTIFYING THE BREAKAGE BEHAVIOUR OF ALUMINA SAMPLES

Ilievski, D*[1], Schibeci, M[2], Livk, I[2]
[1] Alcoa World Alumina, Western Australia
[2]*AJ Parker Centre for Hydrometallurgy & CSIRO Minerals, Australia*

Abstract

To control the breakdown of alumina it is first necessary to understand how an alumina sample breaks, which requires an ability to reproducibly and meaningfully quantify the breakdown behaviour. During the AMIRA P575 project on Alumina Quality, which was sponsored by nine alumina companies and one engineering company, alumina samples from an extensive plant sampling and laboratory program were tested for toughness. To date, the toughness of nearly 50 refinery and laboratory alumina samples has been measured and the samples ranked as being tough or weak. Two interesting observations emerged upon inspecting the raw attrition data and corresponding scanning electron microscopy images of the attrited aluminas:

1. tough and weak aluminas appear to break differently, and
2. certain aluminas classified as tough showed very different breakdown characteristics.

This paper reports on a novel technique, developed at the Parker Centre, for quantifying the breakage behaviour of an alumina sample in terms of the breakdown behaviour of the parent particles (i.e. prior to being subjected to attrition processes) and the daughter particles. The method quantifies the breakage of alumina particles in terms of a breakage rate, daughter particle size distribution after a breakage event, and 'breakage activity' parameter. A key unique feature of the method is that it captures the time-dependent behaviours observed in breakage processes, e.g. the situation where the easier to break structures are broken initially leaving behind progressively stronger particles. A particularly useful feature of the model-based breakage characterization method is its ability to visualise the complex, multi-dimensional information needed to characterise alumina breakage through visualization tools such as 'breakage maps' and 'breakage activity' plots.

The quantitative breakage behaviours of four aluminas, prepared from refinery hydrates, are presented and the results interpreted. Two of the aluminas investigated were classified as tough, one as weak, and the other one as intermediate. The two 'tough' aluminas had very different morphologies and their breakage behaviours were significantly different: one had tougher parent particles but produced weaker daughter particles; one breaks predominantly by a cleavage mechanism whereas the other by a combination of cleavage, chipping and attrition mechanisms. The sample classified as being of 'intermediate' toughness was found to have tough parent particles but weak daughter particles. The sample classified as 'weak' was shown to have weak parent and daughter particles. Attrition is the predominant breakage mechanism for these two samples.

The challenge for the future is to predict breakage behaviour based on the properties of the alumina or pre-cursor hydrate.

1 Introduction

During the AMIRA P575 project on Alumina Quality, and in other investigations, the attrition resistance or toughness has been measured for about 50 refinery and laboratory alumina samples.

The attrition tests were conducted in a modified Forsythe-Hertwig spouted fluid bed and the toughness of the samples was quantified in terms of two parameters: the *k1* parameter, which is a measure of the rate of breakage product particle generation in the important initial stages of attrition; and the *NR1* parameter, which is a measure of the amount of new particles generated during this period.

Alumina samples are classified as strong or tough when both the measured *k1* and *NR1* parameters are low. This can be physically interpreted as the sample having a low rate of breakage fragment generation during the critical initial period, when breakage rates appear to be greatest, and that this period is relatively short leading to relatively few new particles being produced. Conversely, a weak alumina is one where the measured *k1* and *NR1* parameters are high. 'Intermediate' strength alumina samples can either have a low *k1* and a high *NR1* or, alternatively, a high *k1* and a low *NR1*.

Toughness measurements on refinery SGAs showed that the *k1* and *NR1* values were strongly affected by the calcination technology used by the refinery. It was observed that the SGA *k1* values were very similar for a given calcination technology even though the hydrate *k1* values could be very different. To remove the confounding effect of the calciner technology, a laboratory calcination procedure was developed that produced aluminas with similar phase compositions, pore size distributions and specific surface areas (Whittington and Ilievski, 2004).

A number of refinery hydrate samples, from more than 10 refineries world-wide, were calcined using this procedure and the attrition resistance of the resultant laboratory calcined aluminas was measured. A wide range of *k1* and *NR1* values were recorded and the samples were classified as being either tough, weak or of intermediate attrition resistance. Inspection of the number-based particle size distributions at different attrition times and scanning electron microscopy (SEM) images of the attrition products from these samples showed apparent differences in the breakage behaviour. It was observed that tough and weak aluminas appeared to breakdown differently. Also, there were apparent differences in breakage behaviour between certain aluminas

classified as tough. However, these visual observations were qualitative in nature and their usefulness is limited by issues such as representative sampling and count statistics.

To quantitatively investigate the alumina breakdown behaviour, a novel method based on a multi-dimensional population balance equation and utilizing experimental batch attrition and tracer data was developed. This method is briefly described in this paper and its application illustrated using four aluminas prepared from refinery hydrates. The four aluminas comprised of:

Sample A – a tough alumina;
Sample B – also a tough alumina but with a very different morphology and internal structure compared to Sample A;
Sample C – an intermediate alumina;
Sample D – a weak alumina.

The examples are also used to introduce the concepts of 'breakage maps' and 'breakage activity' plots, generated from the model-based breakage characterization method, as aids to help visualize and understand complex multi-dimensional information arising from dynamic particle breakage processes.

2 Characterisation of the four aluminas investigated

A 'Toughness plot' is presented in Figure 1 to show the relative attrition resistances of the four samples in a simple visual form. Samples A and B have low *k1* and *NR1* values. Sample C has a low *k1* and a high *NR1*. Sample D has high *k1* and *NR1* values. The partitions designating the 'Tough', 'Weak' and 'Intermediate' zones in Figure 1 were assigned on the basis of a larger data set (~40 samples) such that >15% of the samples are designate as being 'Tough'.

The *k1* and *NR1* values were also measured for the precursor hydrates of all four samples. The tough alumina samples, i.e. A and B, also had tough precursor hydrates. The precursor hydrates of samples C and D were measured to have similar k1 and NR1 values, indicating that the relative attrition resistance of these two materials changed during calcination.

The morphologies of the four aluminas were quantified from SEM images using the expert system based on the Zaknich image analysis technique (Zaknich, 1997; Roach et al., 1996), and the results are given in Figure 2. The morphology analysis method assigns particles to various categories within five morphology classes, i.e shape, single crystal protrusions, texture, crystallite size and agglomeration. The results can be considered to be a morphology 'fingerprint' of a sample. The four alumina samples show some significantly different morphological features as well as some similarities.

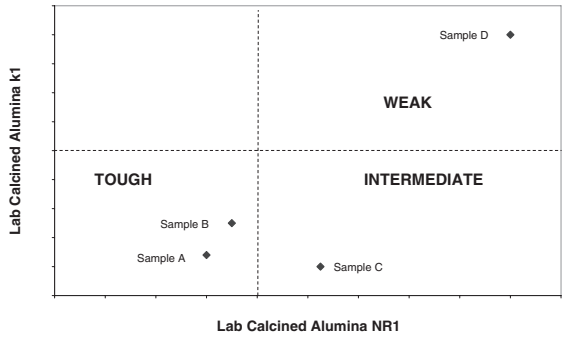

Figure 1. 'Toughness plot' comparing the relative attrition resistances of the four aluminas being investigated.

The mass fraction-based particle size distributions of samples A, C and D were similar. Most of the mass of the samples is distributed between 50 µm and 150 µm. Sample B was coarser, with more +150 µm material.

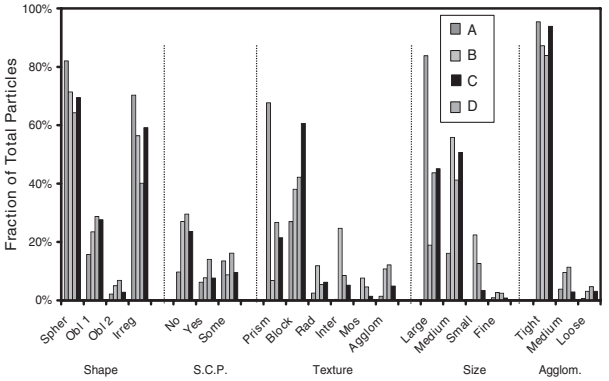

Figure 2. The morphologies of the four alumina samples.

3 Quantitative breakage characterization method description

The quantitative breakage characterisation method consists of two parts: i) generation of breakage data under controlled conditions, which includes measurement of dynamic particle size distribution data (PSD) and dynamic tracer distribution data (TSD), and ii) estimation of breakage parameters using the experimental breakage data and the dynamic 3-D population balance breakage model. A schematic illustrating the procedure is shown in Figure 3.

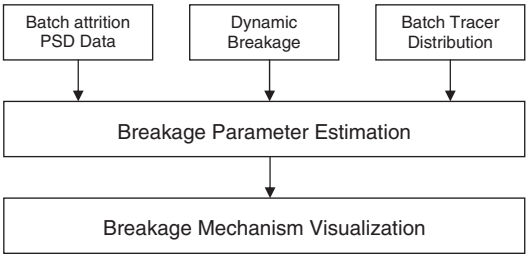

Figure 3. Schematic illustrating the elements of the quantitative breakage characterization method.

(i) Experimental breakage data generation

The breakage was generated using a modified Forsythe-Hertwig spouted bed attrition device with attrition periods ranging from 1–15 minutes. Prior to each attrition test, the material was dry sieved and separated into 6 size-fractions. Particles from each size-fraction were doped with a different tracer element following the procedure developed by Clerin and Laurent (2001); the doping elements were Mo, Co, Cu, Cd and Zn, with the smallest size fraction being left un-doped. After the attrition, the solids were collected and sieved again into the initial size fractions. A small portion of each size fraction was removed and submitted for chemical analysis by ICP to determine the size distribution of the tracer elements. The changes in particle numbers and PSD upon attrition were measured using a Coulter Counter multisizer on samples taken at different attrition times.

(ii) Model-based breakage parameter estimation

A 3-D population balance equation is used to model the breakage process. It describes the changing population distributed with respect to three internal coordinates: parent particle size, particle size at any time and age. The parent particle size coordinate is the size of the pre-attrition or 'parent' particle from which a particle, referred to as the 'daughter' particle, has been generated after a breakage event has occurred. The age coordinate indicates the time since the breakage event that created the particle. The age can also be viewed as a measure of the time spent by a particle in the breakage environment without breaking. It is the introduction of the age coordinate that enables the model to simulate scenarios where the breakage opportunities are changing with time, e.g. the situation where the easier to break structures are removed early from a given size interval leaving only a tougher population.

It is beyond the scope of this paper to describe the development of the complex multi-dimensional equations used to model the breakage processes. Figure 4 is a conceptual representation of the model. The model predicts the size distribution after a given attrition time, tracks the parent particle size interval from which the daughter particles originate, and the time varying breakage activity linked through the age distribution and constitutive equations describing the particle breakage rates.

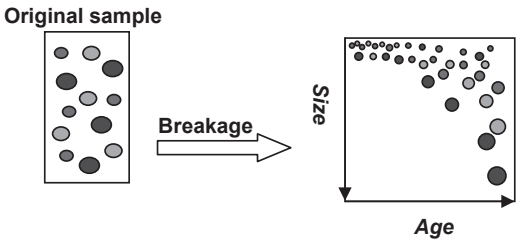

Figure 4. Conceptual model of breakage process; colour depicts the size of original parent particle.

The model is too complex to solve analytically and a numerical solution is required. This was done by converting the continuous form of the population balance model, which is a multi-dimensional partial differential-integral equation, into a series of sets of ordinary differential equations, which can then be solved by standard numerical techniques. This transformation was done by a procedure called discretization (Hill and Ng, 1995).

The breakage model has four sets of breakage parameters: one defining how the breakage rate changes with age, another determining the distribution of daughters upon a breakage event, and two associated with the size dependency of the parent and daughter particle breakage rates. The parameters were estimated by a non-linear parameter estimation, which aims at minimizing the deviation between the model predictions and experimental values of the dynamic PSD and TSD data. A direct search method was used to carry out the optimization.

4 Method validation

The breakage model has been tested by assessing its ability to describe dynamic experimental measurements of:

1. Total particles numbers,
2. Particle size distribution, and
3. Tracer distributions with size.

The results of the latter two tests for one of the alumina samples are presented in Figures 5, (a) shows the evolution of the volume-based PSD after different attrition times, and (b) shows the distribution of the Cu tracer element after 15 minutes of attrition.

The results in Figure 5 show typical level of the agreement observed with the samples analysed to date. These two tests, i.e. to match the breakage PSD and the distribution of the tracer at various attrition times, are particularly challenging. Very good agreement between the model and experimental data has been observed for the 15 alumina samples analysed to date.

5 Quantitative characterization of the breakage behaviour for the 4 alumina samples

The parent particle breakage rates estimated for different alumina samples are presented together in Figure 6. The parent particle breakage rates show a strong particle size dependence. As noted earlier, PSD measurements found that most of the mass in the samples is distributed between the 50 μm and 150 μm size range; the uncertainties in the breakage rate estimates would be lower inside this size range and the estimates more reliable.

Figure 6 shows that the breakage rate of Sample D is significantly larger than the breakage rates of the other three aluminas and Sample B has the lowest parent particle breakage rates.

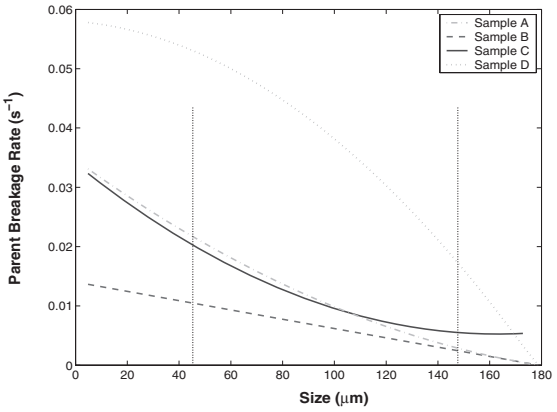

Figure 6. Comparison of the parent particle breakage rates for the four alumina samples. Most of the mass in the samples is distributed between 50 μm and 150 μm, as marked by the vertical dashed lines.

The daughter breakage rates estimated for the four alumina samples are compared in Figure 7. Comparing Figures 6 and 7 it is clear that most daughter particles break more rapidly than parent particles. The daughter particles breakage rates also show less size dependency. The Sample A daughter particle breakage rates are by far the lowest, while the Sample D and Sample C daughter breakage rates are the highest and of a similar magnitude.

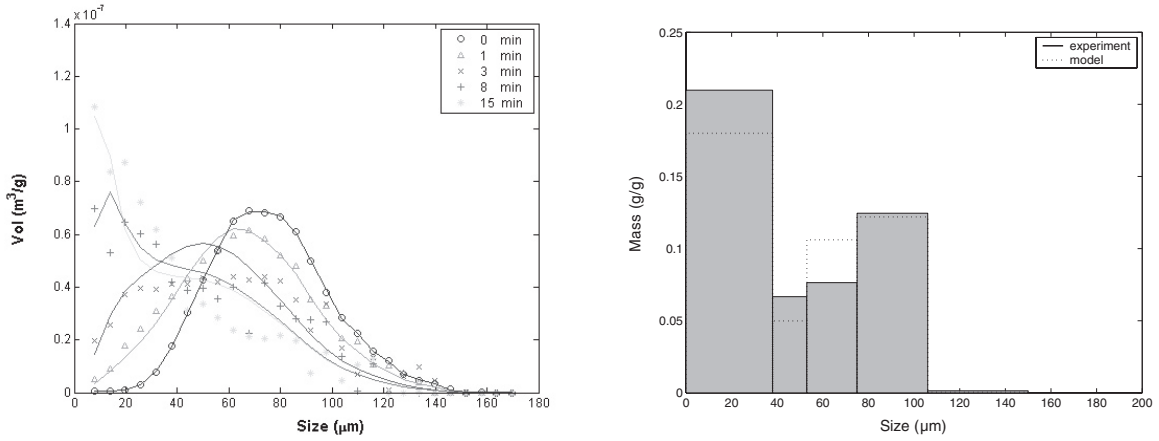

Figure 5. (a) Experimental (symbols) and model predicted (lines) PSD at different attrition times. (b) Experimental and model predicted Cu tracer size distribution after 15 minutes of attrition (Sample D)

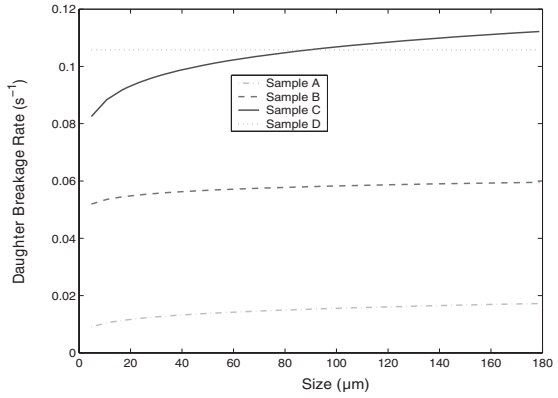

Figure 7. Comparison of the daughter particle breakage rates for the four alumina samples.

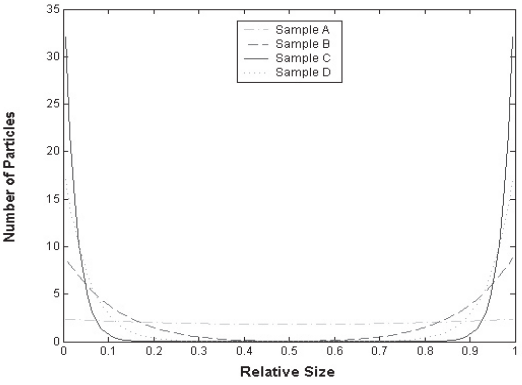

Figure 8. Estimated number-based breakage distribution functions for the four alumina samples.

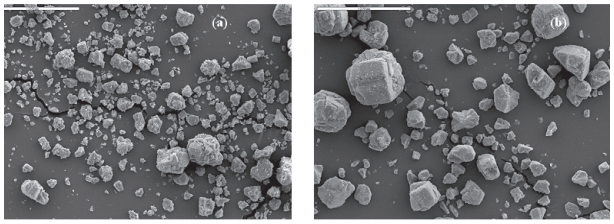

Figure 9. SEM images of the breakage products after 15 minutes in the Hertwig-Forsythe unit for (a) Sample D and (b) Sample A.

Figure 6 and 7 provide an explanation for the toughness ranking of the four samples. Samples A and B are tough because their parent and daughter particle breakage rates are low. Sample A has a higher parent particle breakage rate than Sample B but a lower daughter particle breakage rate. The result is two samples of similar overall toughness. Sample D is weak because both the parent and daughter particle breakage rates are high. Sample C is interesting, its parent particles appear to be as tough as the samples A and B but its daughter particles are very weak leading to it being classified as having intermediate toughness.

An important breakage characteristic of a particulate sample is the breakage distribution function, which describes the distribution of daughter particles arising from a breakage event. Figure 8 gives the estimated breakage distribution functions for the four samples.

Figure 8 shows that samples C and D predominantly break by an attrition or chipping mechanism, producing a combination of fines and particles slightly smaller than the original. In contrast, the breakage product from Sample A is far more evenly distributed, suggesting a cleavage-like mechanism dominates. Sample B is somewhere in between and it is postulated that the attrition, chipping and cleavage mechanisms are present. The results from the quantitative characterization and the postulated breakage mechanisms are consistent with the breakage products observed in SEM images. Figure 9 shows the breakage products for Sample A and Sample D after 15 minutes of attrition. The Sample A particles appear more evenly sized, whereas, Sample D contains significant fines. Pre-attrition SEM images of the samples A and D showed both comprised mostly of larger particles with few fines. However, caution is necessary when attempting quantitative interpretations using SEM images.

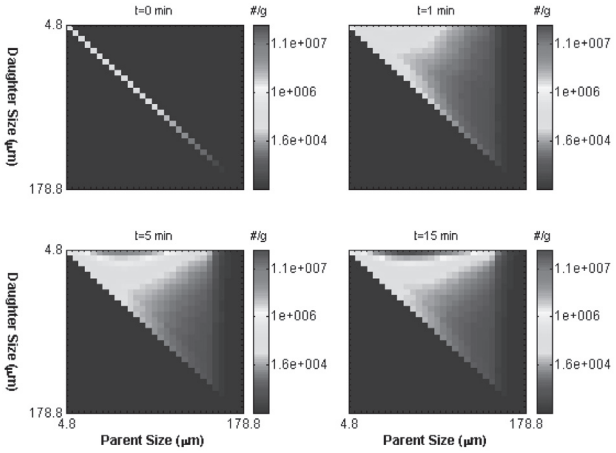

Figure 10. Breakage maps at different attrition times for Sample D, linking the parent size and daughter particle size.

The model-based characterization method can also be used to present an alumina sample's complex breakage characteristics in a variety of graphical forms that help better visualise the breakage behaviour. 'Breakage maps' show the number (or mass) distribution of particles as a function of daughter and parent particle sizes. Figure 10 gives the breakage maps for Sample D at four different attrition times: 0, 1, 5 and 15 minutes. The colour spectrum is a measure of the particle numbers with red indicating the greatest numbers and dark blue representing the nil. The parent particles are represented by the diagonal line at t = 0. The daughter particles originating from a particular parent size are represented by the colours straight up vertically from the diagonal. The lower triangular portion contains no particles as no daughter particles can be bigger than the parent.

The evolution of newly generated particles originating from the various parent particles can be followed by comparing breakage maps at different attrition times. The boomerang-like shape shown in Figure 10 is consistent with an attrition mechanism producing mostly fines and particles slightly smaller than the parent particles. The breakage map for Sample A did not have this form and showed a more uniform distribution.

"Breakage activity" plots are another useful format for visualizing the breakage characteristics. Breakage activity can be interpreted as the rate of generation of new particles and can be expressed using various distributed properties such as number, area or particle volume. Colour is used to indicate the intensity of the breakage activity in a size interval: red corresponding to the size fractions having the greatest propensity to break and blue essentially none. Figure 11 gives the breakage activity plots at different attrition times for sample D, showing the changing PSD on a volume basis superimposed with the changing breakage activities corresponding to each size interval. This figure shows the size intervals that have the greatest propensity to break at any given attrition time. It can be seen the sample progressively becomes deactivated suggesting a situation where most of the opportunities for breakage have been exhausted in the present attrition environment. Breakage activity plots can also be used to follow the breakdown behaviour of a selected size interval, as shown in Figure 12 for a narrow size interval around 60 μm in Sample A. It shows that the daughter particles become progressively deactivated for this sample.

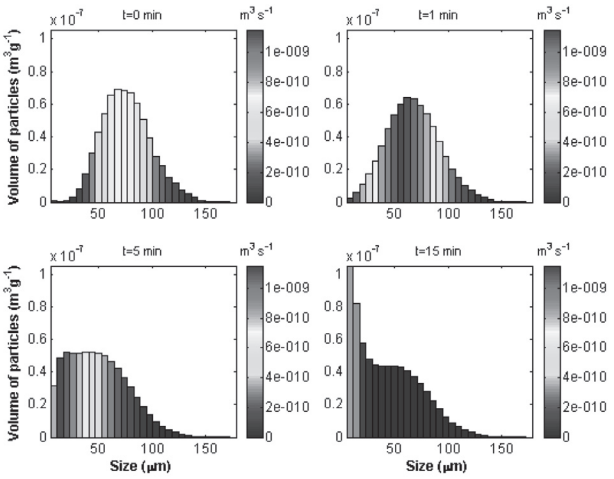

Figure 11. Breakage activity plots at different attrition times for Sample D, showing the changing PSD and the breakage rate intensities within the different size intervals.

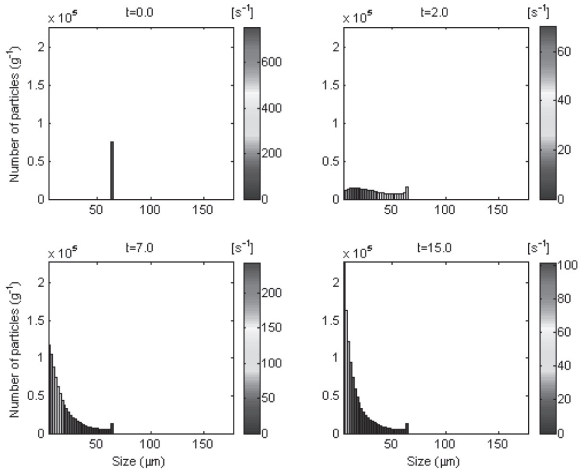

Figure 12. Breakage activity plots at different attrition times for a narrow size interval at 60 µm from Sample A.

6 Conclusions

A method has been presented and validated that quantitatively characterises the breakadown behaviour of alumina particles. The application of the method was illustrated on four aluminas (two tough, one weak and one of intermediate toughness) prepared by laboratory calcining different refinery hydrates. Significant differences in breakage behaviour were observed. The two 'tough' aluminas had very different morphologies and slightly different size distributions. Their breakage behaviours were observed to be significantly different. The parent particle breakage rates were different. However, the sample with the higher parent breakage rates produced very tough daughter particles with very low breakage rates. This sample was shown to break predominantly by a cleavage mechanism whereas for the other sample the daughter breakage rates were higher and breakage appears to be a combination of cleavage, chipping and attrition mechanisms. The sample classified as being of 'intermediate' toughness was found to have tough parent particles but weak daughter particles. The sample classified as 'weak' was shown to have weak parent and daughter particles. Breakage of these two samples was dominated by an attrition mechanism.

Acknowledgements

The authors would like to express their gratitude to the sponsors of the AMIRA 575A project, which has stimulated research innovation over a diverse range of areas. The sponsoring companies at the time of this project were: Alcan, Alcoa, Aughinish Alumina, Comalco, Hydro Aluminium, Outokumpu Technology, Queensland Alumina, BHP Billiton-Worsley, Pechiney and Kaiser.

References

Clerin, P and Laurent, V (2001) 'Alumina Particle Breakage in Attrition Test', Light Metals 2001, pp 41–47.

Hill, PJ and Ng, KM (1995) 'New Discretization Procedure for the Breakage Equation', AIChE J., 41, pp 204–1216.

Roach, G ID and Cornel, JB (1996) 'Alumina and hydrate – unmasking their mysteries eight years on', 4th International Alumina Quality Workshop, Darwin, vol .1, pp 1–8.

Whittington, B and Ilievski, D (2004) 'Determination of the gibbsite dehydration reaction pathway at conditions relevant to Bayer Refineries', Chemical Engineering Journal, 98, pp 89–97.

Zaknich, A. (1997) 'Characterization of aluminium hydroxide particles from the Bayer process using neural network and Bayesian classifiers', IEEE Transactions on Neural Networks, 8(4), pp 919–931.